Polymer Journal, Vol. 33, No. 10, pp 773—782 (2001)

The Hydrogen-Bonding Interactions between 4,4′-Thiodiphenol and Some Poly(hydroxyalkanoic acid)s Revealed by DSC and FT-IR Spectroscopic Analysis

Jianchun LI, Yong HE, Kazuki ISHIDA, Tsuneo YAMANE,* and Yoshio INOUE†

Department of Biomolecular Engineering, Tokyo Institute of Technology, 4259 Nagatsuta, Midori-ku, Yokohama 226–8501, Japan

**Department of Biological Mechanisms and Functions, Graduate School of Bio- and Agro-Sciences, Nagoya University, Chikusa-ku, Nagoya 464–8601, Japan*

(Received May 16, 2001; Accepted July 6, 2001)

ABSTRACT: The specific intermolecular hydrogen-bonding interaction between some poly(hydroxyalkanoic acid)s (PHAs) and 4,4′-thiodiphenol (TDP) were studied by DSC and FT-IR. Chemosynthetic poly(3-hydroxypropionate), bacterial poly(3-hydroxybutyrate-*co*-3-hydroxyvalerate) and bacterial poly(3-hydroxybutyrate-*co*-4-hydroxybutyrate) were used as the PHA samples. A curve-fitting program for line-shape analysis of FT-IR spectra was also applied to investigate the fractions of associated carbonyl groups. The measurements show there are strong intermolecular hydrogen bonds between the carbonyl groups of PHAs and the hydroxyl groups of TDP. The content of intermolecular hydrogen bonds is influenced by both the content of TDP in the PHA/TDP blends and the crystallizability of PHAs. The crystallizability is related to the flexibility of the molecular chains. With the addition of TDP to PHAs, the decrease of melting point T_m and the increase of glass transition temperature T_g of the component of PHAs in the blends were found. When the content of TDP was more than 40%, phase separation took place, which was so serious that T_g dropped obviously as soon as the content of TDP was up to 80%. At this time, it is difficult for the molecules of PHAs and TDP to form intermolecular hydrogen bonds. As indicated by the study of FT-IR, TDP has more ability to form the self-hydrogen-bond of TDP-HO$\cdots$HO-TDP type than the inter-hydrogen-bond of PHA-C=O$\cdots$HO-TDP type. Based on the analysis on the eutectic behavior in different PHA/TDP pairs, it was found that the bulkiness of the pendant alkyl groups in the chains of PHAs affects the eutectic behavior.

KEY WORDS Biodegradable Polyester / Hydrogen Bond / Polymer Blend / Poly(3-hydroxypropionate) / Poly(3-hydroxybutyrate-*co*-4-hydroxybutyrate) / Poly(3-hydroxybutyrate-*co*-3-hydroxyvalerate) / Poly(hydroxyalkanoic acid) / 4,4′-Thiodiphenol /

It is known that the phase behavior of polymer blends is governed by several factors, such as the intermolecular interactions including hydrogen bonds and ion–ion interactions, the molecular weight and polydispersity of the component polymers, the blending process, the thermal history of the blends and so on.[1] Generally speaking, the hydrogen-bonding interaction is much more important compared with the others.

During the past decade the properties of binary blends containing poly(*p*-vinylphenol) (PVPh) have been extensively studied. The hydroxyl groups of PVPh are capable of undergoing intermolecular hydrogen-bonding interactions with proton-accepting functional groups.[2] Since it is well known that the hydroxyl group of the monomeric repeating unit is easily accessible in the *p*-position of aromatic ring, it is not so surprising to find that PVPh is miscible or at least partially miscible over a wide range of composition with the second polymers on the basis of specific hydrogen-bonding interactions, such as polyacrylates,[3] polymethacrylates,[4–11] polyitaconates,[12, 13] polyesters,[14–19] polyethers,[20–23] poly(vinylpyridine)s,[24–27] and poly(1-vinylimidazole).[28] It also has been reported that the addition of PVPh to some immiscible polymer blend systems could improve their miscibility.[29] These studies showed that the favorable hydrogen-bonding interactions are stronger than the dispersing interactions, which may oppose miscibility, and that immiscible blends may be converted to single-phase materials with the introduction of quite low levels of hydrogen bonding.[10]

This phenomenon raises our interest to study whether 4,4′-thiodiphenol (TDP) also have this ability to form intermolecular hydrogen bond with polymers containing carbonyl, ether, ester or other proton-acceptor functional groups, because, as a dihydric phenol, TDP could be thought as the dimer model of PVPh.

On the other hand, it is known that bacterial poly(hydroxyalkanoic acid)s (PHA)s are a family of optically active biodegradable polyesters.[30] The member of this family of thermoplastic biopolymers can show variation in their material properties from rigid

†To whom all correspondence should be addressed (Tel: +81-45-924-5794, Fax: +81-45-924-5827, E-mail: yinoue@bio.titech.ac.jp).

brittle plastics to flexible plastics with good impact properties and to strong tough elastomer, depending on the size and chemical structure of the pendant alkyl group.[31] Nowadays, in industry it is so difficult to find some polymers that are used in pure state, so do PHAs. A variety of additives, such as fillers, plasticizers, age resistances, antioxidants, and so on, are effective to modify the properties of polymeric materials and then to widen greatly their application fields. It would make the problem more complicated because it is unquestionable that not only the properties of these additives but also the different kinds of the pendant alkyl groups are crucial to the properties of the polymer materials. It is necessary to study the influence of some additives, which have the potential ability to form intermolecular interaction with PHAs, on the properties of PHAs with different pendant alkyl groups.

Recently, it has been reported in our previous paper that the addition of TDP to some PHAs, such as poly(3-hydroxybutyrate) [P(3HB)] and poly(3-hydroxybutyrate-*co*-3-hydroxyvalerate) [P(3HB-3HV)] with low content (30 mol%) of 3-hydroxyvalerate (3HV) unit, was an effective way to modify the thermal and mechanical properties of these polyesters.[32]

In this investigation, the changes of thermal properties induced by the intermolecular interaction with TDP are investigated for some PHAs, such as bacterial copolyesters poly(3-hydroxybutyrate-*co*-4-hydroxybutyrate) [P(3HB-*co*-4HB)] with very high 4HB content, bacterial P(3HB-*co*-3HV) with high 3HV content, and chemosynthetic poly(3-hydroxypropionate) [P(3HP)] by differential scanning calorimetry (DSC). Fourier transform infrared spectroscopy (FT-IR), a powerful method to study the intermolecular interaction, is applied to prove the formation of intermolecular hydrogen bonds. These investigations could improve further understanding of the influence of the chemical structure of PHAs on the formation of intermolecular hydrogen bonds with TDP and of the effect of hydrogen bonding interaction on the properties of PHAs.

EXPERIMENTAL

Materials and Preparation of the Blends

The P(3HP) sample ($M_n = 8.12 \times 10^5$, $M_w/M_n = 1.50$) was kindly supplied by Tokuyama Co. (Tsukuba, Japan), which was chemically synthesized through a ring-opening polymerization of propiolactone.

Two P(3HB-*co*-4HB) samples, with 4HB content of 97 mol% [P(3HB-*co*-97 mol%4HB); $M_n = 4.51 \times 10^4$, $M_w/M_n = 1.94$] and of 90 mol% [P(3HB-*co*-90 mol% 4HB); $M_n = 2.75 \times 10^5$, $M_w/M_n = 2.19$] were biosynthesized by fermentation of *Ralstonia eutropha* using the mixture of butyric acid and 4-hydroxybutyric acid as the carbon source.[33] The crude P(3HB-*co*-4HB) were extracted from the dried cells with hot chloroform and purified by precipitation with *n*-heptane. The P(3HB-*co*-3HV) sample with 3HV content of 96 mol% [P(3HB-*co*-96 mol%3HV); $M_n = 2.18 \times 10^5$, $M_w/M_n = 2.41$] was biosynthesized by fermentation of *Paracoccus denitrificans* using *n*-pentanol as carbon source.[34] Biosynthesized P(3HB-*co*-3HV) was extracted from the dried cells with hot chloroform and purified by reprecipitation with chloroform/methanol and chloroform/*n*-hexane systems. The comonomer compositions of all the biosynthesized polyester samples were measured by the ^{1}H NMR spectra in $CDCl_3$ solution on a 270 MHz JEOL GSX-270 NMR spectrometer. ^{1}H chemical shifts were referenced to the signal of tetramethylsilane.

PHA/TDP blend samples containing 0, 10, 20, 30, 40, 60, and 80 wt% of TDP were prepared by casting the mixtures with appropriate ratio of chloroform solution of PHAs (about 2 wt%) and dioxane solution of TDP (about 2 wt%) on the glass petri dishes as the casting surfaces. The films were placed for further 5 days under vacuum at room temperature to eliminate the solvent completely, and at last kept in an oven at 25°C for more than two weeks to allow crystallization of PHAs to approach equilibrium before characterization.

Analytical Procedures

About 5 mg of each sample of PHA blends with different TDP content encapsulated into an aluminum pan was used for measurements of DSC thermograms on a SEIKO-DSC220U. The DSC thermograms were measured by heating from −90 to 200°C at a scanning rate of 20°C min^{-1} (first heating scan). Then, the sample was rapidly quenched to −100°C by liquid nitrogen, and re-heated from −90 to 200°C at a scanning rate of 20°C min^{-1} (second heating scan). Melting point T_m (1st) was taken as endothermic peak top in the thermal diagram recorded by the first heating scan, and heat of fusion ΔH_f (1st) was calculated from the integral of the endothermic melting peak in the DSC curve. Glass transition temperature T_g (2nd) was taken as indicated by DDSC (differentiation of DSC) peak recorded by the second heating scan.

The thin layers of the PHA/TDP blends with a suitable thickness for FT-IR measurements were prepared by casting the PHA/TDP mixtures with appropriate ratio of chloroform solution of PHAs (about 2 wt%) and dioxane solution of TDP (about 2 wt%) on the surface of silicon wafers. The silicon wafer used as a substrate was transparent for an IR incident beam. The maximum

absorption of the resulting thin layer was lower than 1 absorbance unit, which ensured that all absorption was within the linearity range of the detector. The samples were placed for further 5 days under vacuum to eliminate the solvent completely and then kept in an oven two weeks at 25°C. IR measurements were carried out on a single beam IR spectrometer (Perkin–Elmer Spectra 2000) at room temperature under N_2 purging. All spectra were recorded from 600 to 4000 cm^{-1} at a resolution of 4 cm^{-1} and with an accumulation of 64 scans.

A curve-fitting program was applied to resolve the FT-IR carbonyl vibration bands of P(3HB-*co*-4HB) into three components: the amorphous, the crystalline, and the hydrogen-bonded components. This program is based on the least-squares parameter-adjustment criterion using the Gauss–Newton iteration procedure.[35] This fitting adjusts the peak position, the line shape, and peak width and height by a Gaussian-Lorentzian combined line shape function to obtain the best fit.

RESULTS AND DISCUSSION

DSC Analysis on P(3HB-co-97 mol%4HB)/TDP Blends

Differential scanning calorimetry (DSC) analysis is performed in order to study the thermal behavior of the P(3HB-*co*−97 mol%4HB)/TDP blends. Generally, this measurement could supply us some useful information on phase structure of the blends according to the changes of the melting temperature (T_m), glass transition temperature (T_g) and melting enthalpy (ΔH) of the blend components. It is well known that the T_m and ΔH are comparatively easier to be measured from the peak value and the integrated area of the melting peak in the DSC curves, respectively. However, as to the semi-crystalline polymer like some PHAs studied here, the first and the second scans, as described in the experimental part, should be carried out to decrease the influence from the amorphous rigid interfacial region situated between the lamellar crystals and the amorphous phase, which might contain a high fraction of the totally amorphous region and actually it does in this system according to the difference of T_g observed in two scans.

In Figures 1 and 2 are summarized the DSC curves for P(3HB-*co*-97 mol%4HB), TDP and their binary blends in the first and second scans, respectively. The degree of crystallinity of the P(3HB-*co*-4HB) component in the blends could also be estimated from the melting enthalpy, ΔH, in the first scan and the reference melting enthalpy of P(4HB) homopolymer, ΔH_{ref}, *via* $X^* = \Delta H/(0.97 \times W_{4HB} \times \Delta H_{ref})$, where "0.97" represents the weight fraction of the 4HB unit in the P(3HB-*co*-4HB) sample, W_{4HB} is the weight fraction of P(3HB-*co*-4HB) in the blends and ΔH_{ref} = 76 J g^{-1}.[36]

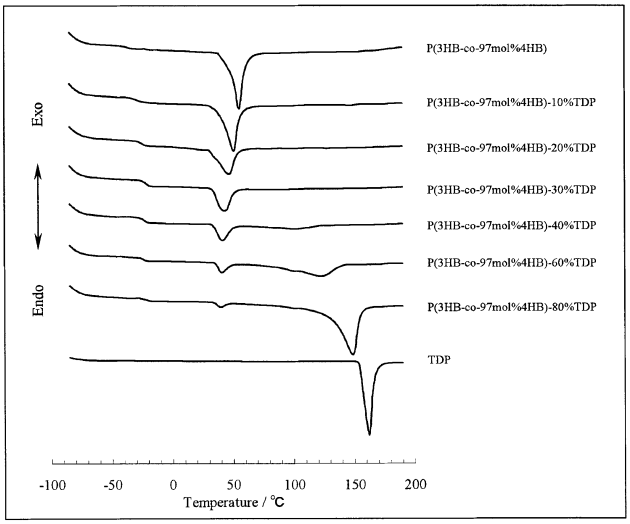

Figure 1. DSC traces of P(3HB-*co*-97 mol%4HB), TDP, and their blends with various TDP contents, recorded during the first heating scan.

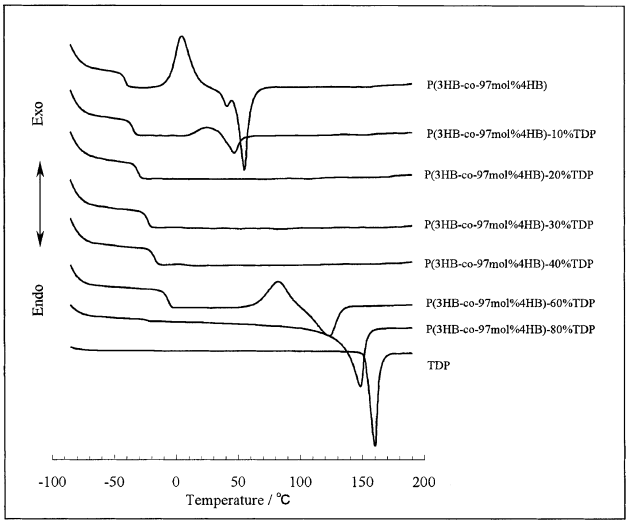

Figure 2. DSC traces of P(3HB-*co*-97 mol%4HB), TDP, and their blends with various TDP contents, recorded during the second heating scan.

The thermal properties of P(3HB-*co*-97 mol%4HB), TDP and their blends are listed in Table I. T_{m1} and T_{m2} are corresponding to the melting temperature of the components of P(3HB-*co*-4HB) and TDP in the blends, respectively. For biosynthesized P(3HB-*co*-4HB)s with wide range of 4HB content, it has been reported that the 3HB component in the copolymer is in the amorphous state when the content of the 4HB unit is more than 70%.[36, 37] According to this result, in the DSC curve of P(3HB-*co*-97 mol%4HB), an endothermic peak appeared at 55.0°C and an increase of heat capacity at −40.8°C should be attributed to the T_m and T_g of the 4HB component in the copolymer. It

Table I. The thermal properties of P(3HB-*co*-97 mol%4HB), TDP, and their blends

Sample	T_{m1}/°C	T_{m2}/°C	Melting Enthalpy/J g^{-1}	Crystallinity/%[a]	T_g/°C
P(3HB-*co*-97 mol%4HB)	55.0	–	43.9	59.5	−40.8
P(3HB-*co*-97 mol%4HB)-10% TDP	50.6	–	37.6	56.7	−34.7
P(3HB-*co*-97 mol%4HB)-20% TDP	45.9	–	24.7	41.9	−30.3
P(3HB-*co*-97 mol%4HB)-30% TDP	42.2	–	19.9	38.6	−22.5
P(3HB-*co*-97 mol%4HB)-40% TDP	41.4	103.9	11.5	26.0	−17.0
P(3HB-*co*-97 mol%4HB)-60% TDP	40.5	122.6	5.6	19.0	−6.0
P(3HB-*co*-97 mol%4HB)-80% TDP	39.2	147.5	1.4	9.5	−22.5
TDP	–	159.7	142.2	–	–

[a]Calculated from the melting enthalpy of the P(4HB) component (the area of the DSC melting peak in the first heating scan), with the melting enthalpy of 100% crystalline P(4HB) assumed to be 76 J g^{-1}.[36]

is obvious that the melting temperature of P(3HB-*co*-97 mol%4HB) component decreases drastically from 55.0°C for pure P(3HB-*co*-4HB) to 39.2°C when the content of TDP in the blends increases up to 80%. At the same time, it is not difficult to find the increasing tendency of T_g of P(3HB-*co*-4HB) with the increase of TDP content. Two points should be emphasized here. At first, what is interesting is that no melting peak corresponding to the TDP component could be observed obviously when the content of TDP in the blends is less than 40% as shown in Figure 1. This might suggest that the TDP component exist in an amorphous state and its crystallization is completely suppressed in the blends. There should be strong intermolecular interaction between P(3HB-*co*-4HB) and TDP, which influences their thermal properties. Furthermore, as mentioned above, although there is an obvious tendency of the increasing T_g of 4HB component with TDP content in the blends even when the TDP content arrives at 60%, the T_g value drops suddenly from −6.0°C to −22.5°C when the content arrives at 80%. It might suggest that at this TDP content serious phase separation take place and it is very difficult for TDP molecules to interact with P(4HB) molecules as a minor component, which is almost in the amorphous state. For the DSC curve of the sample with 80% TDP, an obvious melting peak of TDP component could be observed. For the blend of 60% TDP only a very weak melting peak of TDP is observed. Furthermore, the melting temperature of P(3HB-*co*-4HB) in the blends decreases obviously about 5°C when the content of TDP increases every 10%. However, when the TDP content arrives at about 30% and more, the change of the melting temperature is not so obvious, which keeps almost at 40°C. All these phenomena indicate the fact that the intermolecular hydrogen bonds in the blends, formed between the carbonyl groups of P(3HB-*co*-4HB) and the hydroxyl groups of TDP, make the two components good compatibility when the content of TDP in the blends is not so high. After all, they are different molecules, and the two components in the blends are inclined to be phase separation–one is the P(4HB) crystalline phase and the other is the TDP crystalline phase. When the content of TDP increases to 80%, phase separation becomes the main effect. Hence, the increasing TDP content in the blends does not mean an increasing percentage of the interassociated hydrogen bond between the two components because it is very difficult for TDP, which has its own phase, to form intermolecular hydrogen bonds with P(3HB-*co*-97 mol%4HB), which has also its own phase, when phase separation takes place.

FT-IR Analysis on P(3HB-co-97 mol%4HB), TDP, and Their Blends

FT-IR spectroscopy is a quite suitable technique to investigate the specific intermolecular interaction in the blends. It is well known that if two polymers are completely immiscible, the IR spectrum of the blends is the simple addition of the spectra of two components. The changes of the strength and position of IR absorption peaks resulted from some functional groups characteristics for blend components can be attributed to the existence of intermolecular interactions like hydrogen bonds between the blend components.

The repeating unit, 4HB, has a carbonyl group, yielding a $\nu_{C=O}$ stretching characteristic mode near 1730 cm^{-1}, but the blending partner TDP has no group which shows obvious IR absorption in the region from 1600 to 1850 cm^{-1}. Therefore, it is taken for granted that any changes in the IR spectrum in this region should be directly attributed to the change of the chemical environment of the carbonyl group, such as the formation of hydrogen bonds. On the other hand, every TDP molecule has two hydroxyl groups, which have the ability to form intermolecular hydrogen bonds among TDP molecules themselves. All the hydroxyl groups, including free and hydrogen bonding ones, will induce absorption from 3000 to 3700 cm^{-1} in the IR spectrum. However, there are no hydroxyl groups in the molecular chain of P(3HB-*co*-4HB) except those at the chain terminal of every molecular chain. Considering the mechanism discussed above, this will supply

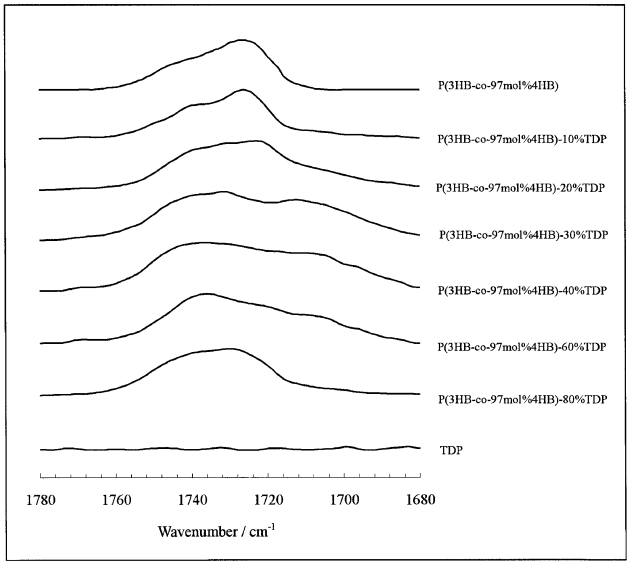

Figure 3. FT-IR spectra in the carbonyl vibration region of P(3HB-*co*-97 mol%4HB), TDP, and their blends with TDP contents from 10% to 80 wt%.

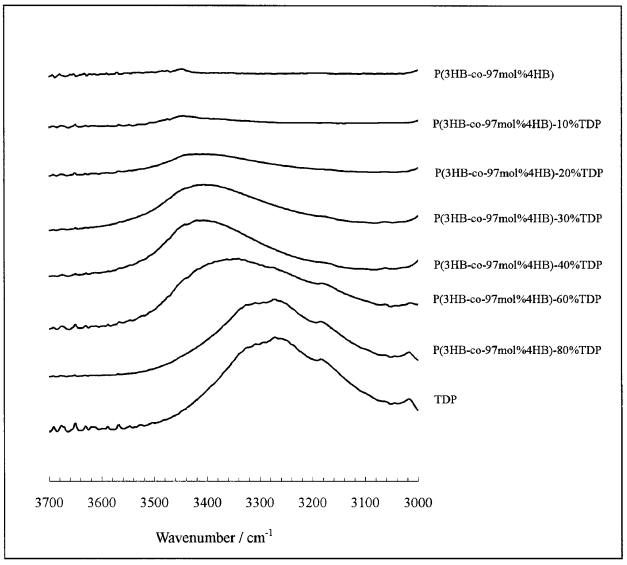

Figure 4. FT-IR spectra in the hydroxyl vibration region of P(3HB-*co*-97 mol%4HB), TDP, and their blends with TDP contents from 10% to 80 wt%.

us additional evidence to confirm the existence of the intermolecular hydrogen-bonding interaction between P(3HB-*co*-4HB) and TDP. At the same time, it will help us to have a further understanding on the competition between the inter-hydrogen-bonding of P(3HB-*co*-4HB)–C=O$\cdots$HO–TDP type and the self- hydrogen-bonding of TDP–C=O$\cdots$HO–TDP type.

In Figure 3 were shown the FT-IR spectra of P(3HB-*co*-97 mol%4HB)/TDP blends in the carbonyl vibration region as the function of TDP composition. When P(3HB-*co*-97 mol%4HB) was blended with TDP, an additional band appeared near a lower wavenumber 1713 cm^{-1} in addition to the band centered on 1730 cm^{-1}, which becomes stronger when increasing the TDP content in the blends. However, when the TDP content is higher than 40%, the relative intensity of this band becomes weaker. When the content arrives at 80%, this band almost disappears. This additional band should be attributed to the vibration for the carbonyl groups with hydrogen bond. It is indicated that, for the blends with low TDP content, the addition of TDP is beneficial to the formation of intermolecular hydrogen bonds between P(3HB-*co*-4HB) and TDP. However, when the content of TDP is more than 40%, there is strong tendency of two components to become phase separation. Phase separation would impede the formation of inter-hydrogen bonds, which is reflected the weakness or disappearance of the band at 1713 cm^{-1} in the IR spectrum. This conclusion is identical to what we obtained from the measurement of DSC.

In Figure 4 is shown the FT-IR spectral changes of P(3HB-*co*-97 mol%4HB)/ TDP blends in the hydroxyl vibration region as the function of TDP composition. In the spectrum of pure TDP, it is obvious that there is a very wide band centered at 3285 cm^{-1}, which should be mainly attributed to the hydroxyl groups in pure TDP. At the same time, in the spectrum for pure P(3HB-*co*-97 mol%4HB), a very weak absorption peak centered at 3455 cm^{-1} was observed in this region and it should be attributed to the vibration of hydroxyl groups at the chain terminal of P(3HB-*co*-4HB). Although it could not be denied that, in the spectra for blend samples, we cannot distinguish between the hydroxyl bands of the P(3HB-*co*-4HB) chains-ends and the TDP molecules, we have enough evidence to consider that contribution to this band from the hydroxyls of P(3HB-*co*-4HB) is negligible. Even to the blend sample with the highest content of P(3HB-*co*-97 mol%4HB) [P(3HB-*co*-4HB)-10% TDP] studied here, the content ratio of hydroxyl groups in the molecules of TDP and in the chain-ends of P(3HB-*co*-97 mol%4HB) is estimated to be only 23.

There are mainly two functional groups, *i.e.*, the carbonyl of P(3HB-*co*-4HB) and the hydroxyl of TDP, which have the ability to take part in the formation of intermolecular hydrogen bonds. TDP has ability to form two kinds of intermolecular hydrogen bonds, *i.e.*, the self-hydrogen-bond of TDP–HO$\cdots$HO–TDP type and the inter-hydrogen-bond of P(3HB-*co*-4HB)–C=O$\cdots$HO–TDP type. It is known that the hydroxyls, which take part in the formation of hydrogen bonds, would produce lower wavenumber absorption in IR spectra, compared with that produced by the hydroxyls, which does not take part in the formation of hydrogen bonds. According to the fact observed in Figure 4 that when the content of TDP decreases, the maximum

peak shifts to higher wavenumber, we know the relative content of hydrogen bonded hydroxyls decreases. However, we cannot distinguish this decrease is mainly induced by the decrease of TDP–HO···HO–TDP type or P(3HB-*co*-4HB)–C=O···HO–TDP type or both of them. The analysis on the carbonyl vibration region has revealed that the content of intermolecular hydrogen bond between P(3HB-*co*-97 mol%4HB) and TDP is highest when the content of TDP is about 40 wt%. It could be concluded that the decrease is induced by TDP–HO···HO–TDP type only and actually the content of P(3HB-*co*-4HB)–C=O···HO–TDP type hydrogen bond increases firstly (when the content of TDP is not less than 40 wt%) and then decreases. With the addition of P(3HB-*co*-97 mol%4HB) to TDP, the relative absorbance of the hydroxyl band decreases and it has the tendency to move to higher wavenumber. The decrease of relative absorbance is induced by the decrease of the content of total hydroxyl groups in the blend systems. It is obvious that TDP has more ability to form the self-hydrogen-bond of TDP–HO···HO–TDP type than the inter-hydrogen-bond of P(3HB-*co*-4HB)–C=O···HO–TDP type.

Quantitative Analysis of the Fractions of Hydrogen-Bonded Carbonyl Groups for P(3HB-co-97 mol%4HB)

Just as discussed above, the analysis of the FT-IR spectra confirmed qualitatively that the intermolecular hydrogen bonds are formed between the carbonyl groups in P(3HB-*co*-4HB) and hydroxyl groups in TDP. Here, the Beer–Lambert law is used to analyze quantitatively the formation of the intermolecular hydrogen bond.[38]

The spectra of P(3HB-*co*-97 mol%4HB) and P(3HB-*co*-97 mol%4HB)-TDP blends in the carbonyl region, which are shown in Figure 3, exhibit two and three distinct components, respectively. The components observed at about 1740.8 and 1725.2 cm^{-1} could be attributed to P(3HB-*co*-97 mol%4HB) in the amorphous and crystalline states, respectively, and that at 1713.0 cm^{-1} to the hydrogen-bonded carbonyl vibration as previously discussed. Here, a curve-fitting program was employed to quantitatively analyze the spectra regarding the integrated intensity of these separated bands.

In Figures 5 and 6 are illustrated the experimental and fitted spectra of pure P(3HB-*co*-97 mol%4HB) and P(3HB-*co*-97 mol%4HB)-40% TDP blend in the carbonyl vibration region, respectively. The experimental spectrum of P(3HB-*co*-97 mol%4HB) was divided into two components, *i.e.*, the amorphous and crystalline bands, while the experimental spectrum for the blend was divided into three components, the amorphous, crystalline, and hydrogen-bonded bands. The good agreement between the experimental and fitted spectra indicates the reliability of this fitting.

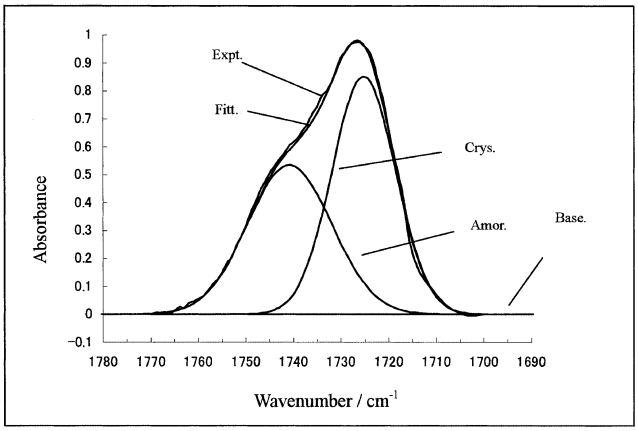

Figure 5. Experimental and fitted spectra for P(3HB-*co*-97 mol%4HB) in the carbonyl vibration region. Expt.: experimental spectrum; Base.: baseline; Amor.: amorphous component; Crys.: crystalline component; Fitt.: fitted spectrum, the sum of the amorphous component and crystalline component.

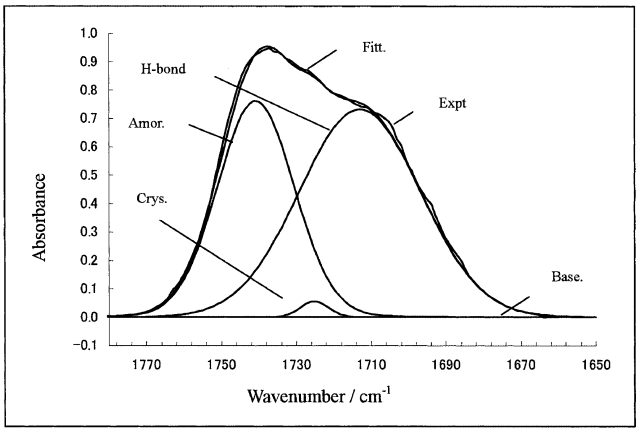

Figure 6. Experimental and fitted spectra for P(3HB-*co*-97 mol%4HB)-40% TDP blend in the carbonyl vibration region. Expt.: experimental spectrum; Base.: baseline; Amor.: amorphous component; Crys.: crystalline component; H-bond.: hydrogen-bonded component; Fitt.: fitted spectrum, the sum of the amorphous component, crystalline component, and hydrogen-bonded component.

According to the Beer–Lambert law, the integrated intensities of the amorphous parts, A_a, the crystalline part, A_c, and the hydrogen-bonded part, A_b, can be expressed as:

$$A_i = TC_i \int_0^{+\infty} \varepsilon_i(\nu)\mathrm{d}\nu \qquad (1)$$

where subscript i represents a, b or c; subscripts a, b, and c are the amorphous, hydrogen-bonded and crystalline carbonyl group parts, respectively; $\varepsilon_i(\nu)$ is the absorption coefficient of i part; T is the thickness; C_i is the concentration of i component; and ν is the wavenumber.

Table II. Fitting results of vibration bands of the carbonyl groups in FT-IR spectra of the blends of P(3HB-*co*-97 mol%4HB) and TDP

Blends	TDP Content / wt%	$A_a/\Sigma A_i$	$A_c/\Sigma A_i$	$A_b/\Sigma A_i$	F_b
P(3HB-*co*-97 mol%4HB)	0	0.45	0.55	0	0
P(3HB-*co*-97 mol%4HB)-10% TDP	10%	0.44	0.41	0.15	0.11
P(3HB-*co*-97 mol%4HB)-20% TDP	20%	0.30	0.31	0.39	0.30
P(3HB-*co*-97 mol%4HB)-30% TDP	30%	0.36	0.01	0.63	0.53
P(3HB-*co*-97 mol%4HB)-40% TDP	40%	0.39	0.01	0.60	0.50
P(3HB-*co*-97 mol%4HB)-60% TDP	60%	0.39	0.22	0.39	0.30
P(3HB-*co*-97 mol%4HB)-80% TDP	80%	0.59	0.27	0.14	0.10

The fraction of hydrogen-bonded carbonyl groups involved in the intermolecular hydrogen bond, F_b, could be calculated according to eq 1:

$$F_b = C_b/(C_b + C_a + C_c) \quad (2)$$

One definition could be made based on eqs. 1 and 2:

$$\gamma_{i/j} = \int_0^{+\infty} \varepsilon_i(\nu)d\nu \Big/ \int_0^{+\infty} \varepsilon_j(\nu)d\nu \quad (3)$$

where subscript j is a, b or c. $\gamma_{i/j}$ is the absorption ratios that take into account the difference between the absorptivities of i and j components. Then F_b can be expressed by A_i and $\gamma_{i/j}$ as:

$$F_b = A_b/(A_b + A_a \times \gamma_{b/a} + A_c \times \gamma_{b/c}) \quad (4)$$

The values of both $\gamma_{B/A}$ and $\gamma_{B/C}$ are estimated to be 1.5, which is comparable to the published data for similar systems.[32, 39, 40] This assumption simplifies the eq 4 to the eq 5:

$$F_b = A_b/(A_b + 1.5A_a + 1.5A_c) \quad (5)$$

Based on the theoretical analysis shown above, in Table II are shown the fitting results and the fractions of hydrogen-bonded carbonyl groups, F_bs, for the P(3HB-*co*-97 mol%4HB)/TDP blends. According to Table II, it is obvious that, with increasing the TDP content, at first the F_b value increases, then arrives at the maximum value when the content of TDP is 30%, and finally decreases. It is indicated that the carbonyl groups of P(3HB-*co*-4HB) and the hydroxyl groups of TDP is inclined to form the intermolecular hydrogen bond at the low TDP content in the blends, however, and at high TDP content, the formation of the intermolecular hydrogen bond is not so easy because of the phase separation between two components.

Effect of Chemical Structure of PHAs on the Thermal Properties of the Blends with TDP

In this section, the thermal properties of the blends of TDP and some other PHAs including P(3HB-*co*-90 mol%4HB), P(3HP), and P(3HB-*co*-96 mol%3HV) are studied.

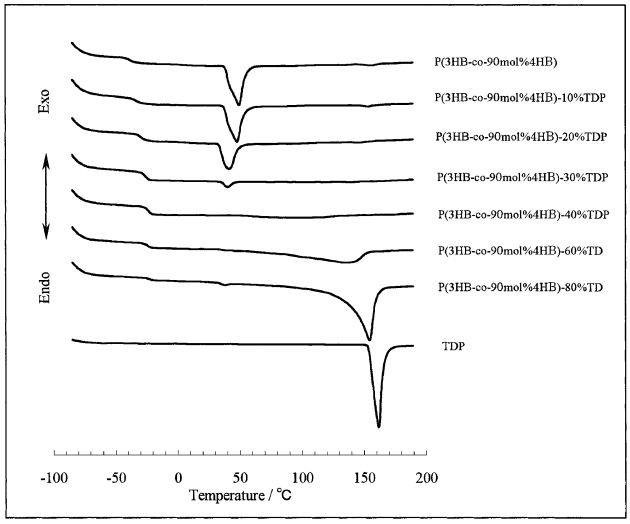

Figure 7. DSC traces of P(3HB-*co*-90 mol%4HB), TDP, and their blends with various TDP contents, recorded during the first heating scan.

In Figure 7 are summarized the DSC curves for P(3HB-*co*-90 mol%4HB), TDP, and their blends in the first scan. Their thermal properties are listed in Table III. T_{m1} and T_{m2} are corresponding to the melting temperature of the P(3HB-*co*-4HB) and TDP components in the blends, respectively. Although the content of the 3HB unit in the copolymer is only 10%, little higher than that in the P(3HB-*co*-97 mol%4HB), it seriously influences the thermal properties of P(3HB-*co*-4HB). At first, the higher content of the 3HB unit in the copolymer leads to the decrease of both the melting temperature and the melting enthalpy of the component of 4HB (Tables I and III). It is indicated that the existence of the 3HB unit does seriously harm to the formation the crystalline phase of P(4HB). Furthermore, the 3HB unit is all in the amorphous state. With the addition of TDP to the copolymer, the tendency of changes of thermal properties is similar to those in the blends of P(3HB-*co*-97 mol%4HB) and TDP. However, comparing the data from two blend systems, it is obvious that the existence of the 3HB unit is beneficial to the formation of intermolecular hydrogen bonds between PHA and TDP. As shown in Figure 2, in the P(3HB-*co*-97 mol%4HB)/TDP blend system, all the components

Table III. The thermal properties of P(3HB-*co*-90 mol%4HB) and its blends with TDP

Sample	T_{m1}/°C	T_{m2}/°C	Melting Enthalpy/Jg^{-1}	Crystallinity/%[a]	T_g/°C
P(3HB-*co*-90 mol%4HB)	49.5	–	28.5	41.7	−38.7
P(3HB-*co*-90 mol%4HB)-10% TDP	48.0	–	24.1	39.1	−35.5
P(3HB-*co*-90 mol%4HB)-20% TDP	41.4	–	17.5	32.0	−30.7
P(3HB-*co*-90 mol%4HB)-30% TDP	40.0	–	2.7	5.6	−23.8
P(3HB-*co*-90 mol%4HB)-40% TDP	–	–	–	–	−18.3
P(3HB-*co*-90 mol%4HB)-60% TDP	–	135.7	–	–	−10.5
P(3HB-*co*-90 mol%4HB)-80% TDP	–	154.5	–	–	−20.6

[a]Calculated from the melting enthalpy of the P(4HB) component (the area of the DSC melting peak in the first heating scan), with the melting enthalpy of 100% crystalline P(4HB) assumed to be 76 J g^{-1}.[36]

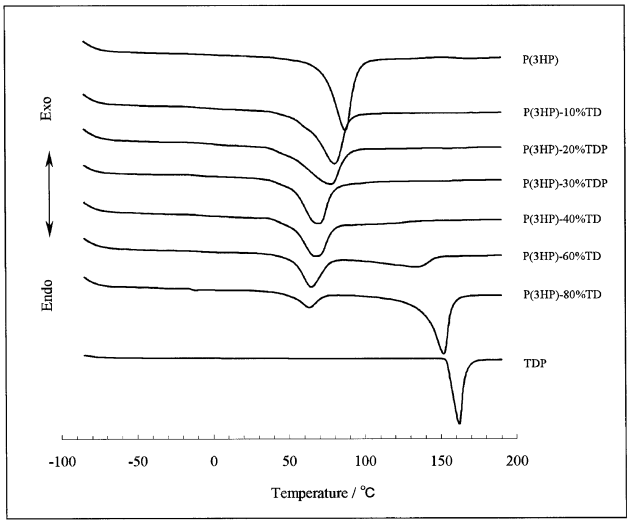

Figure 8. DSC traces of pure P(3HP), TDP, and their blends with various TDP contents, recorded during the first heating scan.

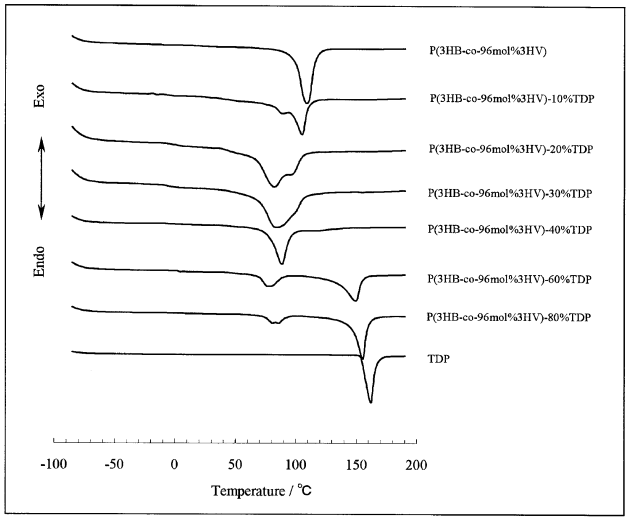

Figure 9. DSC traces of P(3HB-*co*-96 mol%3HV), TDP, and their blends with various TDP content, recorded during the first heating scan.

are in the amorphous state when the content of TDP is 40%, after which phase separation is inclined to take place as discussed above.

In Figure 8 are illustrated the DSC curves for P(3HP), TDP, and their blends in the first scan. It is found that the main features of changes of thermal properties of the blends are similar to those of P(3HB-*co*-97 mol%4HB)/TDP blend system. Although the 3HP and the 4HB units have similar chemical structure, that is, they have no side-chain. The difference in the number of methylene group in the main-chain repeating unit induces two distinct points. The first one is that the melting temperature of P(3HP) gradually but significantly decreases from 87.5°C for pure P(3HP) to 63.2°C when the content of TDP gradually increases up to 80%. However, in the blends of P(3HB-*co*-97 mol%4HB) and TDP, the melting temperature of copolymer component remains almost constant at 40°C when the TDP content is more than 30% (Figure 1 and Table I). It is indicated that phase separation between P(3HP) and TDP is not so serious, which may be beneficial to the formation of intermolecular hydrogen bonds between P(3HP) and TDP. This viewpoint is supported by the analysis of the changes of the melting temperature of TDP component. The second one is that there is a similar trend compared with P(3HB-*co*-4HB), that is, the TDP component is in the amorphous state when the TDP content in the blend is less than 40%, near which content is thought the content of interassociated hydrogen bond becomes the highest. It is explained that both of P(3HP) and P(4HB) are polyesters, the crystallizability of which is seriously influenced by the flexibility of the molecular chain. Because there is one more methylene in the monomeric repeating unit of P(4HB) than in that of P(3HP), it is thought that the P(4HB) chains have better flexibility, which grants P(4HB) more ability to form crystalline phase in the blends. However, since the formation of crystalline phase affects the formation of intermolecular hydrogen bond between polyesters and TDP, it is not so difficult to understand why P(3HP) would have stronger interaction with the TDP molecules.

In Figure 9 are illustrated the DSC curves for P(3HB-*co*-96 mol%3HV), TDP, and their blends in the first scan. When the content of TDP becomes less than 30% in the blends, two melting points clearly appear again. The higher one is attributed to that of the P(3HV)-type

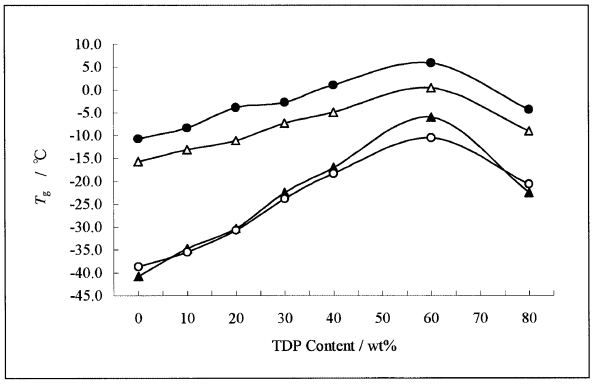

Figure 10. The relationship between glass transition temperatures (T_gs) and TDP content in (▲) P(3HB-*co*-97 mol%4HB)-TDP blends, (○) P(3HB-textitco-90 mol%4HB)-TDP blends, (△) P(3HP)-TDP blends, and (●) P(3HB-*co*-96 mol% 3HV)-TDP blends.

crystalline component and the lower one is thought as the melting of the P(3HB-*co*-96 mol%3HV)/TDP eutectic mixture, which keeps almost constant at about 80°C. Similar eutectic behavior has been found in the P(3HB) and P(3HB-*co*-30 mol%3HV).[32]

It is noteworthy here that the eutectic behavior is observed in the P(3HB)/TDP and P(3HB-*co*-3HV)/TDP blend systems but not in the P(3HB-*co*-97 mol% and 90 mol%4HB)/TDP and P(3HP)/TDP blend systems. It is thought that the existence of the pendant alkyl group, which is inclined to induce the phase separation, has close relationship to the eutectic behavior.

The relationships between glass transition temperatures (T_gs) of polyesters and the TDP content are depicted in Figure 10 for four blend systems investigated in this study. All four curves show the similar tendency of the changes of the T_g value, which at first increases with the increasing TDP content, and then drops when it arrives at 80%. It is thought that the TDP molecules might act as a physical crosslinking agent in the blends because of the intermolecular hydrogen bonds between the carbonyl groups of polyesters and the hydroxyl groups of TDP. It would decrease the flexibility of the polyester chains and increase the glass transition temperatures of the polyester components. When the content of TDP arrives at 80%, very serious phase separation takes place as pointed out above. The content of intermolecular hydrogen bond decreases rapidly, so the T_g decreases to a lower value.

CONCLUSION

As detected by DSC measurements, it is found that intermolecular hydrogen bonds are formed between the carbonyl groups of PHAs and the hydroxyl groups of TDP. The content of intermolecular hydrogen bonds is inclined to increase with the increasing TDP content at first, resulting in the decrease of the T_m value and the increase of the T_g value of PHAs in the blends. When the content of TDP is more than 40%, although phase separation takes place, it could not hinder the tendency of the changes of T_m and T_g. However, as soon as the content of TDP is up to 80%, the phase separation is so serious that T_g drops obviously. At this time, it is difficult for the molecules of PHAs and TDP to form intermolecular hydrogen bonds. As indicated by the study of FT-IR, TDP has more ability to form the self-hydrogen-bond of TDP–HO$\cdots$HO–TDP type than the inter-hydrogen-bond of PHA–C=O$\cdots$HO–TDPtype. The viewpoint of phase separation is supported by the line-shape analysis of FT-IR spectra using the curve-fitting program. With increasing the TDP content, at first the F_b value increases, then arrives at the maximum value when the content of TDP is 30% , and finally decreases.

The study of the influence of chemical structure of PHAs on the formation of intermolecular hydrogen bond indicates that the flexibility of molecular chains would affect the crystallizability of PHAs and affect the formation of intermolecular hydrogen bonds with TDP because of the phase separation. Based on the analysis on the eutectic behavior in different PHAs/TDP pairs, it is thought that the pendant alkyl groups in the chains of PHAs, the existence of which is inclined to induce the phase separation, have close relationship to the eutectic behavior.

Acknowledgments. This work was partly supported by a Grant-in-Aid for Scientific Research on Priority Area, "Sustainable Biodegradable Plastics", No. 11217204 (2000) from the Ministry of Education, Culture, Sports, Science and Technology (Japan).

REFERENCES

1. J. W. Barlow and D. R. Paul, *Polym. Eng. Sci.*, **21**, 985 (1981).
2. S. H. Goh, S. Y. Lee, Y. T. Yeo, X. Zhou, and K. L. Tan, *Macromol. Rapid Commun.*, **20**, 148 (1999).
3. M. M. Coleman, A. M. Lichkus, and P. C. Painter, *Macromolecules*, **22**, 586 (1989).
4. S. H. Goh and K. S. Siow, *Polym. Bull.*, **17**, 453 (1987).
5. C. J. T. Landry and D. M. Teegarden, *Macromolecules*, **24**, 4310 (1991).
6. C. J. Serman, P. C. Painter, and M. M. Coleman, *Polymer*, **32**, 1049 (1991).
7. J. A. Pomposo, I. Eguiazabal, E. Calahorra, and M. Cortazar, *Polymer*, **34**, 95 (1993).
8. J. A. Pomposo, M. Cortazar, and E. Calahorra, *Macromolecules*, **27**, 245 (1994).
9. D. Li and J. Brisson, *Macromolecules*, **30**, 8425 (1997).

10. J. Dong, and Y. Ozaki, *Macromolecules*, **30**, 286 (1997).
11. D. Li and J. Brisson, *Macromolecules*, **29**, 868 (1996).
12. C. J. T. Landry, B. K. Coltrain, D. M. Teegarden, and W. T. Ferrar, *Macromolecules*, **26**, 5543 (1993).
13. J. Hong, S. H. Goh, S. Y. Lee, and K. S. Siow, *Polymer*, **36**, 143 (1995).
14. L. A. Belfiore, C. Qin, E. Ueda, and A. T. N. Pires, *J. Polym. Sci., Part B: Polym. Phys.*, **31**, 409 (1993).
15. C. J. T. Landry, D. J. Massa, D. M. Teegarden, M. R. Landry, P. M. Hendrichs, R. H. Colby, and T. E. Long, *Macromolecules*, **26**, 6299 (1993).
16. H. L. Chen, S. F. Wang, and T. L. Lin, *Macromolecules*, **31**, 8924 (1998).
17. L. L. Zhang, S. H. Goh, and S. Y. Lee, *J. Appl. Polym. Sci.*, **70**, 811 (1998).
18. P. X. Xing, L. S. Dong, Y. X. An, Z. L. Feng, M. Avella, and E. Martuscelli, *Macromolecules*, **30**, 2726 (1997).
19. P. Iriondo, J. J. Iruin, and M. J. Fernandez-Berridi, *Macromolecules*, **29**, 5605 (1996).
20. P. Pedrosa, J. A. Pomposo, E. Calahorra, and M. Cortazar, *Macromolecules*, **27**, 102 (1994).
21. X. Zhang, K. Takegoshi, and K. Hikichi, *Macromolecules*, **26**, 2198 (1993).
22. C. J. Serman, Y. Xu, P. C. Painter, and M. M. Coleman, *Polymer*, **32**, 516 (1991).
23. I. Akiba and S. Akiyama, *Polym. Networks & Blends*, **7**, 147 (1997).
24. M. Vivas de Maftahi and J. M. Frechet, *Polym. J.*, **29**, 477 (1988).
25. J. Y. Lee, E. J. Moskala, P. C. Painter, and M. M. Coleman, *Appl. Spectrosc.*, **40**, 991 (1986).
26. J. Dai, S. H. Goh, S. Y. Lee, and K. S. Siow, *Polym. J.*, **26**, 905 (1994).
27. X. Zhou, S. H. Goh, S. Lee, and K. L. Tan, *Appl. Surf. Sci.*, **119**, 60 (1997).
28. S. H. Goh, S. Y. Lee, and L. I. T. Tan, *Polym. Bull.*, **37**, 253 (1996).
29. M. Hosokawa and S. Akiyama, *Polym. J.*, **31**, 13 (1999).
30. A. J. Anderson and E. A. Dawes, *Microbiol. Rev.*, **54**, 450 (1990).
31. H. Brandl, R. A. Gross, R. W. Lenz, and R. C. Fuller, *Adv. Biochem. Eng. Biotechnol.*, **41**, 77 (1990).
32. Y. He, N. Asakawa, and Y. Inoue, *J. Polym. Sci., Part B: Polym. Phys.*, **38**, 2891 (2000).
33. H. Kimura, T. Ohura, M. Takeishi, S. Nakamura, and Y. Doi, *Polym. Int.*, **48**, 1073 (1999).
34. T. Yamane, X. F. Chen, and S. Ueda, *Appl. Environ. Microbiol.*, **62**, 380 (1996).
35. Y. He and Y. Inoue, *Polym. Int.*, **49**, 623 (2000).
36. H. Mitomo, W. C. Hsieh, K. Nishiwaki, K. Kasuya, and Y. Doi, *Polymer*, **42**, 3455 (2001).
37. H. Mitomo, N. Morishita, and Y. Doi, *Rep. Prog. Polym. Phys. Jpn.*, **7**, 671 (1994).
38. A. Sanchis, M. G. Prolongo, C.Salom, and M. R. Masegossa, *J. Polym. Sci., Part B: Polym. Phys.*, **36**, 95 (1998).
39. D. Li and J. Brisson, *Polymer*, **39**, 793 (1998).
40. D. Li and J. Brisson, *Polymer*, **39**, 801 (1998).